

# EFFECTS OF ENERGY DEPOSITION MODELS AND CONDUCTIVE COOLING ON WIRE SCANNER THERMAL LOAD, ANALYTICAL AND FINITE ELEMENT ANALYSIS APPROACH

B. Cheymol\*, European Spallation Source, Lund, Sweden

## INTRODUCTION

A number of wire scanners will be installed in the ESS linac [1] to measure beam profile and perform emittance measurement with a 3-gradients type method. The ESS wire scanner will be equipped with 33  $\mu\text{m}$  for carbon wire in the warm linac and a 40  $\mu\text{m}$  for tungsten wire in the cold linac.

Due to the high power on the beam, the duty cycle has to be reduced to allow the insertion of interceptive devices, preliminary estimations of the wire thermal load [2] show that the wire can withstand the 2 dedicated modes:

- A slow tuning mode (i.e. 50  $\mu\text{s}$ , up to 62.5 mA, 1 Hz).
- A fast tuning mode (i.e. 10  $\mu\text{s}$ , up to 62.5 mA, 14 Hz).

The temperatures have been estimated with a simple analytical model assuming no conductivity effect, the energy deposited in the wire has been estimated with the stopping power extracted from table and assuming a constant thickness of the wire equal to its diameter, this paper proposes to update the estimation of the wire temperature with different model for the energy deposition and to compare the results of the analytical model to the results of a Finite Element (FE) analysis. In all the document, the beam intensity is equal to 65 mA.

## ANALYTICAL MODEL PARAMETERS

The thermal load on wire induced by the beam could in the worst case damage the wire. Given a linac pulse, populated by  $N_{part}$  particles with RMS transverse beam sizes  $\sigma_x$  and  $\sigma_y$ , traversing a wire, the induced temperature can be calculated as:

$$\Delta T = \frac{N_{part}}{\rho C_p(T)V} \frac{\Delta E}{2\pi\sigma_x\sigma_y} e^{-\left(\frac{x^2}{2\sigma_x^2} + \frac{y^2}{2\sigma_y^2}\right)} \quad (1)$$

Where  $C_p(T)$  is the specific heat capacity of the material of the wire,  $\rho$  is the wire material density and  $V$  volume of the wire and  $\Delta E$  the energy deposited in the wire per particle.

### Wire Material Properties

An analytical model of the specific heat capacity of the carbon and of the tungsten has been used for the estimation of the temperature, data can be found in [3] and [4]. The density of the materials (respectively 1.8  $\text{g}\cdot\text{cm}^{-3}$  for carbon and 19.25  $\text{g}\cdot\text{cm}^{-3}$  for tungsten) as well as the emissivity (0.8 for carbon and 0.1 for tungsten) were assumed to be independent of the temperature in a first approximation.

\* benjamin.cheymol@esss.se

## Cooling Process

In first approximation, the conductive cooling is negligible, thus it is assumed that the wire cooling is dominated by black body radiation, described by Stefan-Boltzmann law. The heat radiated from the wire surface is proportional to the fourth power of the temperature. The difference from the ideal black-body radiation is described by a factor called emissivity and the radiated power is given by :

$$P = \sigma \varepsilon A (T^4 - T_0^4) \quad (2)$$

Where  $\sigma$  is the Stefan-Boltzmann constant,  $\varepsilon$  the emissivity,  $A$  the area of the body,  $T$  its temperature and  $T_0$  the ambient temperature (set in all the studies presented in the document at 298 K). After a linac pulse the temperature variation can be calculated as:

$$\frac{dT}{dt} = \frac{\sigma \varepsilon A (T^4 - T_0^4)}{\rho C_p(T)V} \quad (3)$$

Other processes like thermoionic emission or wire sublimation are more efficient at high temperature, nevertheless for the ESS wire scanners and in general for wire scanners (or SEM grid) use at low energy beam, the thermoionic emission will perturb the signal from secondary emission. The wire temperature shall be kept below 2000 K to avoid this effect, thus these processes are neglected in this note.

## Energy Deposition Models

The energy deposited per particle has been estimated with the stopping power extracted from tables and the length of interaction assuming a constant stopping power across the wire diameter. For low beam energy, the stopping power increases when the particles move into the wire material. Assuming a constant stopping power, calculated for the incident beam energy leads to underestimation of the deposited energy.

For simplification, in the analytical model, the energy deposited by each particle crossing the wire is identical. This assumption leads to error due to the cylindrical geometry of the wire if the wire diameter is taken as interaction length. To reduce this error, an equivalent thickness of the wire can be calculated as:

$$e_{equ.} = \frac{\pi d}{4} \quad (4)$$

where  $d$  is the wire diameter.

The equivalent thickness of the wire is reduced by  $\approx 25\%$  compared to the wire diameter, the energy deposition is

reduced by the same fraction, both calculations of the deposited energy have been used for the estimation of the wire temperature.

The energy deposited per particle in the wire has been also estimated with the Monte Carlo code FLUKA [5], for beam energies from few MeVs to 2 GeV. The results is normalized by primary in the simulations and allows a direct comparison with the previous method.

The comparisons between the models are shown in Fig. 1 and Fig. 2 for both wire considered in the ESS linac, the energy deposited calculated for interaction length equal to the wire diameter is taken as a reference.

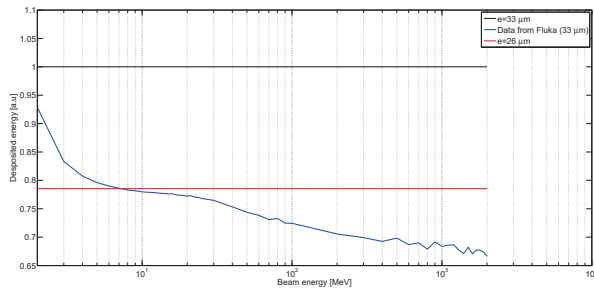


Figure 1: Normalized energy deposition on a 33  $\mu\text{m}$  carbon wire as function of the beam energy estimated with stopping power table (black and red curve) and by a Monte Carlo code (blue curve).

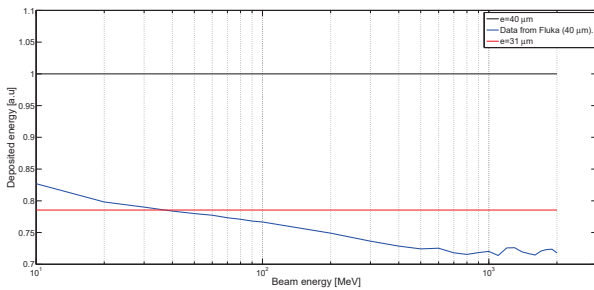


Figure 2: Normalized energy deposition on a 40  $\mu\text{m}$  tungsten wire as function of the beam energy estimated with stopping power table (black and red curve) and by a Monte Carlo code (blue curve).

Compared to the reference, the estimation of the energy deposited with an equivalent thickness is almost 25 % lower. At low energy, the results from the Monte Carlo code is higher than the results of estimation with the tables, this is mainly due to the assumption of a constant stopping power. For the high energies, the results from the Monte Carlo simulations show a reduction of the deposited energy of almost 35 % for a carbon wire and almost 30 % for a tungsten wire compare to the reference. Due to the limitations of the code, the energy deposited might be even lower. FLUKA is not able to track electrons below 1 keV, thus, the low energy tail of  $\delta$ -rays spectra might be counted in the energy deposition while in reality some of them will escape the wire and not contribute to the thermal load.

ISBN 978-3-95450-178-6

## ESTIMATION OF THE TEMPERATURE WITH THE ANALYTICAL MODEL

The wire temperature has been estimated using an analytical model and for the 3 energy deposition models for the higher thermal load in the ESS linac, for carbon wire, the worst case is the first wire scanner in MEBT ( $E_{\text{beam}} = 3.63 \text{ MeV}$ ,  $\sigma_x = 1.85 \text{ mm}$ ,  $\sigma_y = 1.45 \text{ mm}$ ) and for tungsten wire, the worst case is the WS installed in the LEDP ( $E_{\text{beam}} = 90 \text{ MeV}$ ,  $\sigma_x = 2.6 \text{ mm}$ ,  $\sigma_y = 1.8 \text{ mm}$ ).

All simulations have been performed assuming a pulse length of 100  $\mu\text{s}$  at a repetition rate of 1 Hz. The temperature on the wire has been calculated for 10 consecutive pulses, with the wire centered in the beam. The results are presented in Fig. 3 to Fig. 4.

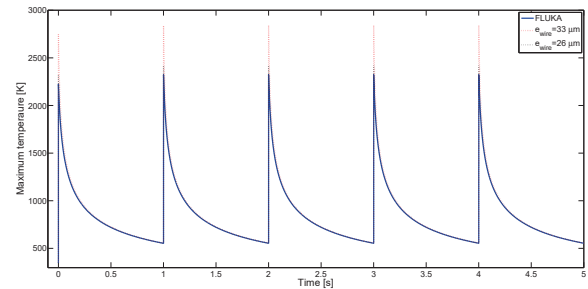


Figure 3: Peak temperature evolution as function of the energy deposited for a wire scanner in the MEBT, beam pulse is 100  $\mu\text{s}$  (33  $\mu\text{m}$  carbon wire).

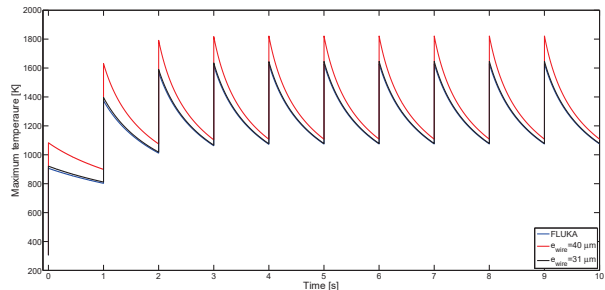


Figure 4: Peak temperature evolution as function of the energy deposited for a wire scanner installed in the LEDP, beam energy is 90 MeV (40  $\mu\text{m}$  tungsten wire).

Up to 90 MeV beam, for all wire considered, the difference between the results given by the Monte Carlo code and the analytical model using an equivalent thickness are negligible. At higher energy the difference between the models appears more clearly, the difference is about 50 K between FLUKA and the equivalent thickness. Considering the full wire diameter lead to an error about 500 K in the worst case and about 100 K for the 2 GeV case (see Fig. 5).

## COMPARISON WITH FINITE ELEMENT ANALYSIS

In the analytical model, the conduction is neglected, this might be a good assumption for a carbon wire due to the

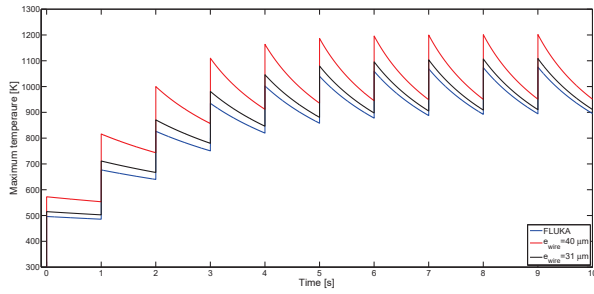


Figure 5: Peak temperature evolution as function of the energy deposited for a wire scanner installed at the linac end, beam energy is 2000 MeV, beam sizes are equal to 2 mm in both planes (20  $\mu\text{m}$  tungsten wire)

high emissivity of the material, but for a tungsten wire, the emissivity is almost an order magnitude lower and its thermal conductivity is higher, the conduction might not be negligible and can be the main contributor of the cooling process.

In order to estimate the influence of thermal conductivity on the wire temperature, it has been decided to perform a series of simulation with the Finite Element code ANSYS®.

### Finite Element Model

From the energy deposition estimated with the Monte Carlo code FLUKA, a 3D map of the heat generation (in  $\text{W}\cdot\text{m}^{-3}$ ) has been generated for different beam energies, beam sizes and wire type. Then, these maps have used as an input in ANSYS to calculate the wire temperature. The exact wire properties are not know, the ANSYS model has been fed with the properties of pure tungsten (data can be found at [4]) and the properties of the R4550 graphite. The emissivity of these two material was assumed to be constant. The temperature at the wire ends has been fixed in the model to 298 K, the ambient temperature is set at the same value.

### Carbon Wire

The beam parameters used to generate the 3D maps are shown in Table 1, the parameters have been chosen in order to have a case with a maximum temperature around 2000 K and one case with a maximum temperature equal to approximately 700 K without stopping power gradient along the beam path. The maximum temperature evolutions for both cases and for the analytical and FE models are shown in Fig. 6 and Fig. 7.

Table 1: Beam Parameters Used to Generate the 3D Heat Generation Maps for the 33  $\mu\text{m}$  Carbon Wire.

Energy [MeV]	$\sigma_x$ [mm]	$\sigma_y$ [mm]
20	1	1
200	1	1

For the 20 MeV case, the agreement between the 2 models is good, the temperature after the first pulse is approximately the same (1695 K for the analytical model and 1665 K for the

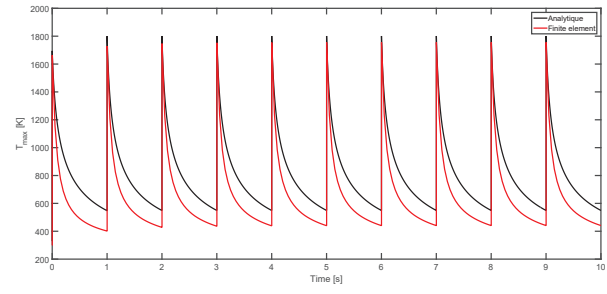


Figure 6: Evolution of the peak temperature estimated with an analytical model (blue curve) and a FE model (red curve), the beam energy is 20 MeV (33  $\mu\text{m}$  carbon wire).

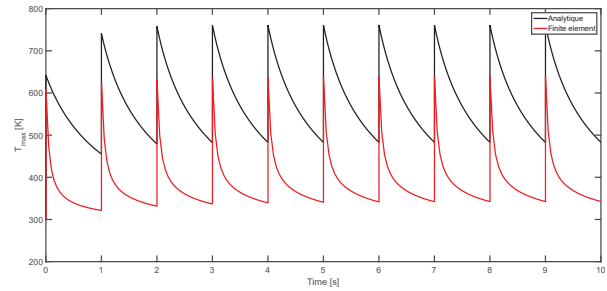


Figure 7: Evolution of the peak temperature estimated with an analytical model (black curve) and a FE model (red curve), the beam energy is 200 MeV (33  $\mu\text{m}$  carbon wire).

FE model). The cooling is more efficient in the FE model, after the first period of cooling, the temperature is 547 K in the analytical model and 401 K in the FE model. The maximum temperature over the 10 pulses are also similar (1801 K in the analytical model and 1756 K in the FE model), the error between the models is approximately 3 %.

For the 200 MeV case, if the temperature after the first pulse is similar for both models ( $\approx 620$  K), the difference after the first cooling period is around 150 K and the maximum temperature over the 10 pulses shows a difference of 33 % (760 K in the analytical model and 638 K in the FE model). The analytical model over estimate the temperature, this is might due to the small radiation cooling efficiency for temperature below 800 K. In order to check the effect of the different cooling processes, the radiation and conductivity have been alternatively which off in the FE code <sup>1</sup>. The results of the 20 MeV case are shown in Fig 8 and Tab 2.

Table 2: Temperature on 33  $\mu\text{m}$  Carbon Wire for a 20 MeV Beam With  $\sigma_x = \sigma_y = 1$  mm Estimated With different Models.

	Analytical	FE model		
Radiation	on	on	on	off
Conductivity	off	on	off	on
$T_m$ 1 pulse [K]	1695	1665	1665	1665
$T_m$ [K]	1801	1756	1938	2623

<sup>1</sup> For this, the material thermal conductivity has been reduce by 6 orders of magnitude in the material properties

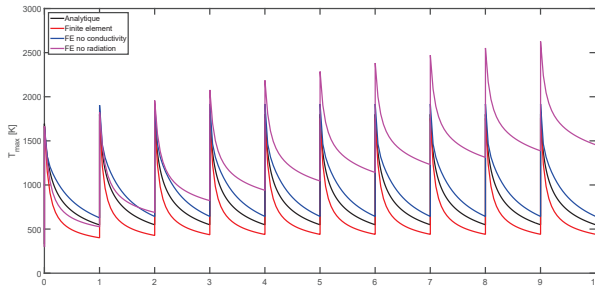


Figure 8: Comparison of different FE models for a 20 MeV beam and a 33  $\mu\text{m}$  carbon wire.

The temperature after the first pulse is similar in all the cases (error  $\approx 2\%$ ) and identical in all the FE models. without radiation cooling activated, the temperature is not stabilized after 10 pulses, the difference is above 800 K compare to full FE model. If the conductive cooling is not activated in the FE model, the equilibrium is reached after couple of pulses, a similar evolution as the analytical mode. From the results it seems that the analytical model overestimated the radiation cooling, the estimated maximum temperature in this case is 9 % lower.

Similar conclusions can be made for the low temperature case, the analytical model overestimated the radiation cooling, without conduction, the 2 models (FE and analytical) are in good agreement, nevertheless in this range of temperature, thermal conductivity can not be neglected.

For all results presented in this subsection, it is interesting to note that the temperature close to wire ends is still at 298 K after 10 seconds.

### Tungsten Wire

Similar studies has been performed for a 40  $\mu\text{m}$  tungsten wire, the beam parameters used for the 3D maps generation are presented in Table 3, these parameters have been chosen in order to be in the same temperature range as the carbon wire example.

Table 3: Beam Parameters Used to Generate the 3D Heat Generation Maps for the 40  $\mu\text{m}$  Tungsten Wire

Energy [MeV]	$\sigma_x$ [mm]	$\sigma_y$ [mm]
200	1	1
2000	2	2

As shown in Fig. 9 and in Table 4 for the high temperature case, the FE model without thermal conduction activated and the analytical model show similar behavior as what was seen for the carbon wire case in particular an overestimation of the radiative cooling in the analytical model.

With conduction activated, the cooling is more efficient, the maximum temperature is 700 K lower after the first cooling period. The maximum temperature over 10 seconds is almost 20 % lower compare to the analytical model, in this model the equilibrium is reach faster than the FE model.

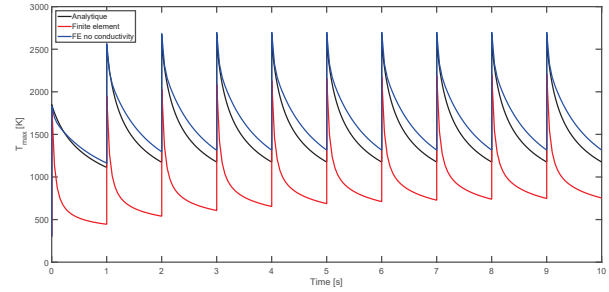


Figure 9: Evolution of the peak temperature for different FE models and on a 40  $\mu\text{m}$  tungsten wire for a 200 MeV beam.

Table 4: Temperature on 40  $\mu\text{m}$  Tungsten Wire for a 200 MeV Beam With  $\sigma_x = \sigma_y = 1$  mm Estimated With Different Models.

	Analytical	FE model	
Radiation	on	on	on
Conductivity	off	on	off
$T_{max}$ [K]	2573	2210	2701
$T_{max}$ at 1 second [K]	1112	445	1162

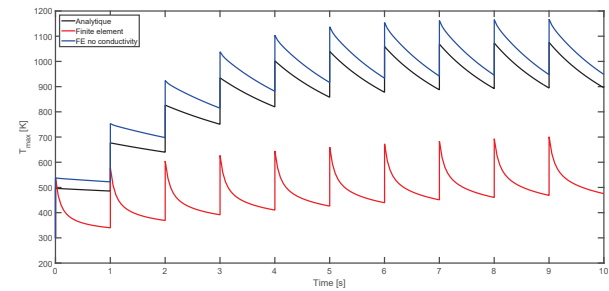


Figure 10: Evolution of the peak temperature for different FE models and on a 40  $\mu\text{m}$  tungsten wire for a 2000 MeV beam.

For a lower thermal load on the wire (i.e. the 2000 MeV case), these discrepancies between the models are higher as shown in Fig. 10. With lower temperature after the first pulse, the radiation cooling is not efficient and there is almost no cooling process, this clearly appears in the analytical model and in the FE model with conductivity non activated. The models are not converging and the difference on the peak temperature between the full FE model and the analytical model is up to a factor 2 at the equilibrium,

The analytical model for a tungsten wire does not seem to be accurate for low duty cycle and low thermal load. To confirm the behavior of a tungsten wire, another series of simulations with the fast mode scan parameters (i.e. 14 Hz, 10  $\mu\text{s}$ ) have been performed with the same e beam parameters (see Table 3).

As shown in Fig. 11 for the 200 MeV, the temperature is stabilizes only if the conduction is not activated in the models, for the full FE model, after 29 pulse, the equilibrium is not reached, the maximum temperature for the models are summarized in Table 5. The radiation cooling seems



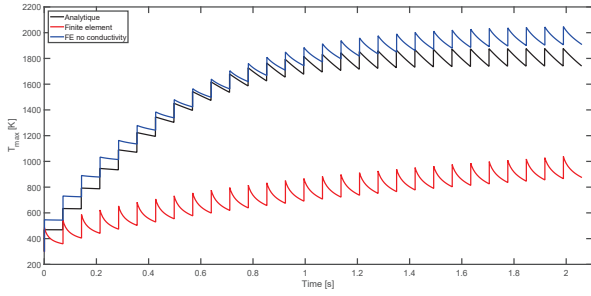


Figure 11: Evolution of the peak temperature for different FE models and on a 40  $\mu\text{m}$  tungsten wire for a 200 MeV beam, during a fast mode scan.

to be efficient if the temperature is above 500 K. The peak temperature is reduce by a factor 2 in the full FE model compare to the analytical model, this is similar to what was seen in the previous set of simulations.

Table 5: Temperature on 40  $\mu\text{m}$  Tungsten Wire for a 200 MeV Beam With  $\sigma_x = \sigma_y = 1 \text{ mm}$  in Fast Mode.

	Analytical	FE model	
Radiation	on	on	on
Conductivity	off	on	off
$T_{max} \text{ [K]}$	1878	1038	2048

At 2000 MeV, with lower thermal load, a similar behavior of the different models can be seen in Fig. 12. The equilibrium is not reach for all models, and it appears clearly that the analytical model overestimates the radiation cooling at low temperature, but the estimated temperature is at least a factor 2.5 higher than the full FE model.

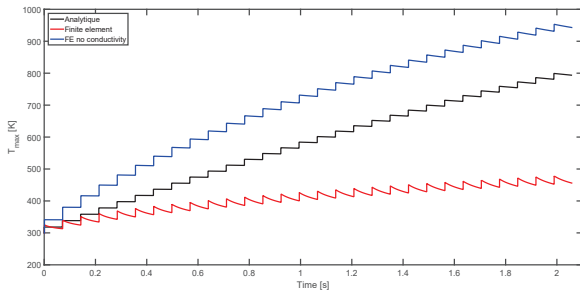


Figure 12: Evolution of the peak temperature for different FE models and on a 40  $\mu\text{m}$  tungsten wire for a 2000 MeV beam, during a fast mode scan.

Like the carbon wire case, the temperature close to the wire end remains at 298 K after the last pulse.

## CONCLUSION

It is often written in the literature that the conductivity can be neglected to estimate the thermal load on a thin wire.

From the simulations performed for this note, it can be concluded that this statement is true only for a thin carbon wire operating at high temperature. For tungsten wire and operation at low temperature, the simple analytical model without conductivity is valid only to estimate with enough accuracy the temperature rise after a single shot.

The analytical model seems valid for high emissivity material and high temperature operation, domain where the radiation cooling is the most effective. Outside this domain, using a simple analytical model can lead to an overestimation to the wire temperature by 33 % for a carbon wire and by up to a factor 2.5 for tungsten wire compare to a full treatment of the cooling processes. Nevertheless, it must be noted that the thermal properties of the wire material are not well known, the results presented in this note might a best case scenario. Some discrepancy between the material thermal properties used in the FE model and the "real" wire properties might occur.

It would be interesting to perform a series of tests with a tungsten wire to validate the results of the FE model or update the thermal properties of a tungsten filament.

Assuming a best case scenario from the FE model, if the difference for carbon wire can be neglected during a design phase, the difference for a tungsten wire might induce some over constraints on machines parameters during operation of the interceptive devices.

For an accelerator like ESS, with a very high beam power density, the machine operation is not constraint by this overestimation of the wire temperature, the temperature after a single shot is high enough to neglect the thermal conductivity, in most of the case simulated for the ESS wire scanner, the temperature is above 1200 K after a single shot.

For accelerators with lower beam power density, the temperature after a single shot might below few hundred of Kelvins, and thus be outside the domain of validity of the analytical mode, for these cases a full FE model is be mandatory to estimate the maximum duty cycle which the wire can withstand.

## REFERENCES

- [1] M. Eshraqi *et al.*, "The ESS Linac", in *Proc. IPAC'14*, Dresden, Germany, THPME043.
- [2] B. Cheymol, "Thermal load and signal level of the ESS wire scanner" in *Proc. LINAC'14*, Geneva, Switzerland, MOPP036,
- [3] M. Plum, "Wire scanner and harp signal levels in the SNS", SNS Technical Note SNS 104050200-TD0023 - R00.
- [4] <http://aries.ucsd.edu/LIB/PROPS/PANOS/>
- [5] A. Ferrari, P.R. Sala, A. Fasso, and J. Ranft, "FLUKA: a multi-particle transport code" CERN-2005-10 (2005), INFN/TC\_05/11, SLAC-R-773.